

Article

In-Situ Generation of Brønsted Acidity in the Pd-I Bifunctional Catalysts for Selective Reductive Etherification of Carbonyl Compounds at Mild Conditions

Dan WU, Willinton Yesid Hernandez, Songwei Zhang, Evgeny I. Vovk,
Xiaohong Zhou, Yong Yang, Andrei Y Khodakov, and Vitaly V. Ordomsky

ACS Catal., **Just Accepted Manuscript** • DOI: 10.1021/acscatal.8b04925 • Publication Date (Web): 21 Feb 2019

Downloaded from <http://pubs.acs.org> on February 21, 2019

Just Accepted

"Just Accepted" manuscripts have been peer-reviewed and accepted for publication. They are posted online prior to technical editing, formatting for publication and author proofing. The American Chemical Society provides "Just Accepted" as a service to the research community to expedite the dissemination of scientific material as soon as possible after acceptance. "Just Accepted" manuscripts appear in full in PDF format accompanied by an HTML abstract. "Just Accepted" manuscripts have been fully peer reviewed, but should not be considered the official version of record. They are citable by the Digital Object Identifier (DOI®). "Just Accepted" is an optional service offered to authors. Therefore, the "Just Accepted" Web site may not include all articles that will be published in the journal. After a manuscript is technically edited and formatted, it will be removed from the "Just Accepted" Web site and published as an ASAP article. Note that technical editing may introduce minor changes to the manuscript text and/or graphics which could affect content, and all legal disclaimers and ethical guidelines that apply to the journal pertain. ACS cannot be held responsible for errors or consequences arising from the use of information contained in these "Just Accepted" manuscripts.



ACS Publications

is published by the American Chemical Society, 1155 Sixteenth Street N.W.,
Washington, DC 20036

Published by American Chemical Society. Copyright © American Chemical Society.
However, no copyright claim is made to original U.S. Government works, or works
produced by employees of any Commonwealth realm Crown government in the course
of their duties.

In-Situ Generation of Brønsted Acidity in the Pd-I Bifunctional Catalysts for Selective Reductive Etherification of Carbonyl Compounds at Mild Conditions

Dan Wu,^{a,b} Willinton Y. Hernández,^a Songwei Zhang,^c Evgeny I. Vovk,^c Xiaohong Zhou,

^c Yong Yang,^c Andrei Y. Khodakov,^{b} and Vitaly V. Ordomsky^{a, b*}*

^a Eco-Efficient Products and Processes Laboratory (E2P2L), UMI 3464 CNRS-Solvay,

201108 Shanghai, People's Republic of China, E-mail : vitaly.ordomsky-ext@solvay.com;

^b Univ. Lille, CNRS, Centrale Lille, ENSCL, Univ. Artois, UMR 8181 – UCCS – Unité de

Catalyse et Chimie du Solide, F-59000 Lille, France, E-mail : [andrei.khodakov@univ-](mailto:andrei.khodakov@univ-lille.fr)

lille.fr;

^c School of Physical Science and Technology, Shanghai Tech University, Shanghai

201210, People's Republic of China.

ABSTRACT. Selective synthesis of ethers from biomass-derived carbonyl compounds is an important academic and industrial challenge. The existing processes based on strong acid or metallic catalysts cannot provide high selectivity to ethers due to the occurrence of side reactions. Hereby we propose a Pd-I bifunctional heterogeneous catalyst for selective reductive etherification of aldehydes with alcohols. Extensive catalyst characterizations uncovered the presence of iodine species on the surface of Pd nanoparticles. Heterolytic dissociation of hydrogen on the I-Pd surface sites leads to the “in-situ” generation of Brönsted acidity, which promotes reaction toward corresponding ethers with extremely high selectivity at very mild reaction conditions.

KEYWORDS. Acidity generation, Surface modification, Palladium and iodine, Reductive etherification, Biomass upgrading.

1
2
3
4
5
6
7
8
9
10
11
12
13
14
15
16
17
18
19
20
21
22
23
24
25
26
27
28
29
30
31
32
33
34
35
36
37
38
39
40
41
42
43
44
45
46
47
48
49
50
51
52
53
54
55
56
57
58
59
60

Introduction

Ethers and its derivatives are widely used as solvent, surfactants, pharmaceuticals, polymers and liquid fuels [1-3]. Traditional routes for the synthesis of ethers normally involve dehydration of alcohols over mineral acids or heterogeneous polymer Nafion-H at

1
2
3 elevated temperatures ($>150\text{ }^{\circ}\text{C}$) [4-6]. The Williamson ether synthesis by reaction of
4
5
6
7 alcohol with an alkyl halide is another possible approach for the ether production [7-8].
8
9
10 However, this reaction requires synthesis of environmentally harmful halides as
11
12
13 intermediates.
14
15
16

17 The selectivity is the most important challenge in the synthesis of ethers from
18
19
20 biomass-derived feedstocks. The reaction selectivity is usually insufficient in the
21
22
23 traditional synthesis routes, because of complex structure of the biomass-derived
24
25
26 substrates, which simultaneously contain several functional groups like carbonyls and
27
28
29 hydroxyls. The reductive condensation of alcohols with aldehydes and ketones yielding
30
31
32 ethers has been recently proposed as an innovative route to valorize bio-sourced platform
33
34
35 molecules [9-11]. The reaction mechanism involves intermediate acetalization of carbonyl
36
37
38 group over an acid catalyst with subsequent hydrogenolysis of the reaction intermediates
39
40
41 to ethers over metal sites. For example, combination of Pt and Amberlyst-15 has been
42
43
44 used for transformation of 5-(hydroxymethyl)furfural (HMF) to 2,5-bis(alkoxymethyl)furan
45
46
47 with an yield close to 60 % [9]. The proximity of acid and metal sites in the bifunctional
48
49
50 metal-acid catalysts is commonly enhanced by using liquid acids or their solutions (H_2SO_4 ,
51
52
53
54
55
56
57
58
59
60

HCl etc) [12]. Recently metal chlorides have been proposed for this reaction as catalysts combining both hydrogenation and acidic properties [13]. Beside acetalization and hydrogenolysis reaction pathway, another option was using Lewis acid zeolite such as Sn-Beta or Zr-Beta, where reaction involves transfer hydrogenation of HMF to 2,5-bis(hydroxymethyl)furan (BHMF) followed by etherification [14-15]. However, poor selectivity, high temperature, low catalytic activity and difficult catalyst separation from the reaction products have been so far serious drawbacks for the implementation of reductive etherification in an industrial scale. In another report, with generation of PdH species as acid sites during hydrogenation reaction, Pd on carbon with 0.7% loading is able to catalyze furfural reductive etherification to furfuryl ethyl ether in ethanol with 81% yield [16]. However, this process suffers from narrow reaction temperature windows, limitation of substrates and catalyst degradation.

Molecular iodine has been reported as an effective catalyst for the acetalization reactions, which has been widely used as a protection method for the carbonyl groups in organic synthesis [17-18]. One of possible catalytic effects of iodine is related to the generation of hydrogen iodide, which acts in liquid solutions as a Brönsted acid and

1
2
3 activates the carbonyl groups by hydrogen bonding effects [19-20]. Recently, surface
4
5
6
7 modification of heterogeneous catalysts, which often results in major enhancement in
8
9
10 chemoselectivities in numerous reactions, has gained significant interests [21-23].
11
12
13 Modification of metal-supported catalysts with iodine could be therefore, favorable for the
14
15
16
17 selective synthesis of ethers from aldehydes and alcohols, since both acetalization and
18
19
20 hydrogenolysis functions will be combined in proximity over a single catalyst. However,
21
22
23 this strategy of catalyst design has not yet been explored given the well-known strong
24
25
26
27 poisoning effect of iodine on metal catalysts such as Pt, Au and Pd [24-25].
28
29
30

31 Herein, we developed an extremely efficient Pd-I catalyst ([Figure 1](#)) for reductive
32
33
34 condensation of aldehydes and ketones with alcohols with high ether productivity and
35
36
37 operating at very mild reaction conditions. The catalyst described in this work can be
38
39
40 prepared by “in situ” modification of a commercially available Pd-supported catalyst with
41
42
43
44 organic iodide. This substantially simplifies its preparation process.
45
46
47
48
49
50
51

52 Experimental section

53 54 55 *Catalyst Preparation*

5 wt. % of Pd on alumina or carbon supports (Pd/Al₂O₃ or Pd/C, Johnson Matthey) has been used as a parent catalyst. Deposition of iodine on the surface of Pd has been performed by addition of 0.2 g of Pd/Al₂O₃ or Pd/C together with 50 mg of ethyl iodide (EtI) in 6 g of isopropanol into 40 ml stainless-steel reactor. The reactor was pressurized with 10 bar of H₂ and stirred at 60 °C for 1 h. Afterwards, the catalyst has been separated and thoroughly washed with isopropanol and dried in the vacuum oven at 80 °C overnight. The synthesized samples were denoted as I-Pd/C and I-Pd/Al₂O₃. Preparation methods of other iodine modified catalysts like I-Pd/Al₂O₃ (N₂), NaI-Pd/Al₂O₃, I₂-Pd/Al₂O₃ and I₂/Al₂O₃ are specified in Supporting Information (SI).

Characterization

For TEM analysis, a JEOL-2011F having an acceleration voltage of 200 kV was used. Prior to TEM characterization, the samples were dispersed in ethanol solution with ultrasonic treatment for 30 min and then dropped onto a carbon film on copper grid. The content of iodine in I-Pd/Al₂O₃ catalyst was determined by Energy Dispersive Spectroscopy (EDS) analysis.

XPS analysis has been performed in a ThermoFischer ESCALAB 250Xi photoelectron spectrometer using monochromated X-ray irradiation Al K α ($h\nu = 1486.7$ eV) and 180° double focusing hemispherical analyzer with a six-channel detector. The BE (binding energy) of the photoemission spectra was calibrated to Al 2p peak with BE 74.5 eV for Al containing samples and to adventitious carbon C 1s peak with BE 284.8 eV for PdI₂.

The CO pulse adsorption was performed using AutoChem II 2920 apparatus from Micromeritics. 50 mg of sample was put in a quartz reactor, and then the samples were reduced in a flow of 5% H₂/Ar flow (60 ml/min) with heating rate 10 °C/min at 60 °C for 0.5 h. After cooling down to 45 °C the catalyst has been treated by CO pulses in He flow till full saturation. H₂-TPR

has been performed in the same unit using CryoCooler for sub-ambient (-70 °C) measurements with heating rate 10 °C/min in 5% H₂/Ar flow.

FTIR spectra were recorded using a Thermo Fisher Scientific Nicolet 6700 FTIR (32 scans at a resolution of 4 cm⁻¹) equipped with a mercury cadmium telluride (MCT) detector. Pyridine and CO-FTIR experiments were performed in a vacuum cell (less than 10⁻⁵ torr). The catalyst samples for analysis were pressed in a 40 ~ 50 mg/cm² (D=13 mm) self-supporting discs. Before analysis, all samples were reduced at 60 °C for 1 h with subsequent vacuum treatment for 3 h. CO adsorption has been performed by addition of CO doses in the cell at r.t. till full saturation of the signal. Pyridine (Py) adsorption has been performed in the same way by addition of Py doses. For some experiments 500 torr of hydrogen has been introduced in the cell after Py adsorption.

Catalysis

The etherification reaction has been conducted in a 40 ml stainless-steel autoclave equipped with a magnetic stirrer, pressure gauge and an automatic temperature controller. In a typical experiment, 2 g of isopropanol, 0.1 g of furfural and 50 mg of catalyst with or without 15 mg of organic iodide were loaded into reactor. Afterwards, the reactor was sealed and pressurized by 20 bar of H₂, followed by heating up to the target temperature with continuous magnetic stirring. After reaction, the autoclave was cooled down, the pressure was released and the solution was separated by filtration and analyzed by gas chromatography (GC) with biphenyl as the internal standard. In some experiments, other alcohols and carbonyl compounds have been used instead of furfural and isopropanol.

The products of the reaction have been analyzed by GC (Agilent Technologies 7820A) equipped with a polar column of HP-5 and flame ionization detector (FID), with inlet temperature of 250 °C. The products have been separated by starting from 75 °C and hold for 5 min with

subsequent heating to 260 °C with the rate 10 °C/min. GC-MS analysis (Agilent Technologies 5977A MSD with Agilent Technologies 7890B GC system equipped with HP-5 capillary column) was used to identify the organic compounds.

The conversion of carbonyl compound, selectivity and yield to corresponding products were defined as follows:

$$\text{Conversion (\%)} = 1 - \frac{n_A}{n_A^0}$$

$$\text{Selectivity to the product p (\%)} = \frac{n_p}{n_A^0 - n_A}$$

$$\text{Yield (\%)} = \text{Conversion} \times \text{Selectivity}$$

n_A , n_A^0 and n_p refers to the final, initial moles of carbonyl compound and final moles of product, respectively. Biphenyl was used as internal standard for the GC analysis.

Results and discussion

Etherification over the Pd-I catalysts

The commercial catalyst Pd/Al₂O₃ (5 wt. %) has been used for hydrogenation of furfural in isopropanol solution. The catalyst demonstrated high activity with formation of tetrahydrofurfuryl alcohol (THFA) as the main product ([Table 1, Entry 1](#)). Addition of traces of ethyl iodide (EtI) in the reactor leads to a total change of the reaction route ([Table 1, Entry 2](#)), causing a favored formation of ether (2-(isopropoxymethyl)furan) as the main

product (91.8 % selectivity) and traces of acetal (2-(diisopropoxymethyl)furan). Note that this dramatic change in the selectivity could be explained either by the presence of EtI as co-catalyst during the reaction, for example, by generation of HI or as modifier of the Pd-supported catalyst.

In order to identify the role of EtI, we did the treatment of Pd/Al₂O₃ with EtI in isopropanol solution, at the reaction conditions, but without furfural. Afterwards, the solid catalyst was washed thoroughly with isopropanol and dried in vacuum oven overnight to remove the physically adsorbed iodine species. The modified I-Pd/Al₂O₃ catalyst demonstrated lower catalytic activity compared with the mixed system Pd/Al₂O₃ and EtI but showed very similar selectivity towards formation of the ether ([Table 1, Entry 3](#)).

Another indication on modification of the catalyst by iodine species is in its stable catalytic performance after 5 cycles with intermediate separation by centrifugation and addition of fresh substrate without EtI ([Figure S1, SI](#)). Comparable reaction rates were observed in several consecutive reaction cycles ([Figure 2](#)). The decline of selectivity after 15 min of test for 2 and 3 cycles could be explained by accumulation of water in the catalyst leading to higher formation of hemiacetal at the initial stage of the reaction.

In order to check the role of hydrogen in the genesis of active sites, we have performed the treatment of Pd/Al₂O₃ by EtI in inert atmosphere of nitrogen. The catalyst demonstrates the catalytic performance similar to initial Pd/Al₂O₃ catalyst with THFA as the main product of the reaction (92.6 %, [Table 1, Entry 4](#)). Thus, hydrogen atmosphere is necessary for the effective modification of the palladium catalyst.

In order to verify the role of iodine species on the catalytic performance we have performed modification of the catalyst by the NaI salt which resulted only in partial catalyst deactivation without affecting the selectivity observed for non-promoted Pd/Al₂O₃ catalyst ([Table 1, Entry 5](#)). Thus, the modification of the catalyst might be explained by reaction of Pd with organic iodide in the presence of hydrogen with formation of atomic iodine on the surface. Numerous previous studies demonstrated that alkyl iodides could dissociate on metal surface with generation of iodine atoms and alkanes species in the presence of H₂ [26]. To confirm the dissociation of alkyl iodides, isobutyl iodide (iBuI) and iodobenzene (IBn) were also used as iodine source in the reaction mixture. Notably, high yield of ether ([Table 1, Entry 6 & 7](#)) was observed in both experiments. Moreover, the analysis of the products from Pd/Al₂O₃ promoted with IBn had shown the presence of benzene in the products ([Figure S2, SI](#)). This indicates on the dissociation of IBn with formation of iodine species, which might modify the Pd catalyst. Moreover, the iodine molecule has been also used as an additive ([Table 1, Entry 8](#)). Although the

1
2
3 formation of ether was observed in the products, conversion of furfural was quite low. The main
4
5 side product was acetal due to the presence of I_2 in the reaction mixture, which is well known as a
6
7 catalyst for acetalization reaction. However, the catalyst pretreated by molecular I_2 in isopropanol
8
9 solution has demonstrated relatively high activity and selectivity to ether (**Table 1, Entry 9**). It has
10
11 been reported that I_2 can dissociate on the metal surface with formation of adsorbed iodine atoms
12
13 [27]. Thus, organic iodides as well as molecular iodine can be used for modification of the surface
14
15 of Pd.
16
17

18
19 Note that iodine could modify both the alumina support and Pd. In order to verify the role of
20
21 support in this reaction we have tested Pd/C (5 wt. % Pd) in hydrogenation of furfural in the
22
23 presence of EtI (**Table 1, Entry 10-11**). The non-promoted Pd/C catalyst demonstrated high
24
25 selectivity to THFA similar to Pd/ Al_2O_3 . However, additionally the catalyst yields 2-
26
27 methyltetrahydrofuran as the product of deeper hydrogenation and tetrahydropyran derivatives as
28
29 the products of ring opening and re-cyclization (**Figure S3 & Table S2, SI**). High activity of Pd/C
30
31 catalyst in deep hydrogenation reactions has been explained earlier by inert support and presence
32
33 of unsaturated sites over Pd nanoparticles [28-29]. Similar to the alumina supported catalyst,
34
35 promotion of Pd/C with EtI also shifts the selectivity of the reaction towards the ether. The same
36
37 effect is also observed after pre-treatment of the Pd/C catalyst by EtI (**Table 1, Entry 12**). It
38
39 means that the pre-treatment of alumina with iodide does not play a key role in the modification
40
41 of the selectivity of the reaction.
42
43
44
45

46
47 Non-supported Pd powder was tested in this reaction as well (**Table 1, Entry 13 & 14**). In
48
49 the presence of traces of EtI, the selectivity to ether increased from 0 to 33.3 %. The low conversion
50
51 of furfural on non-supported Pd resulted from the low metal surface area (**Table S1, SI**). These
52
53 results indicate that iodine most probably modifies Pd, leading to the new active species for
54
55
56
57
58
59
60

selective synthesis of ether. In this case, the formation of PdI_2 could be responsible for change of the reaction route. Test of PdI_2 salt in the reaction has shown formation of acetal as the main product of the reaction without ether in the products (**Table 1, Entry 15**). The absence of ether could be explained by absence of metallic sites for acetal hydrogenolysis.

Iodine molecule itself has been shown earlier as an active catalyst in transformation of aldehydes [17]. We have checked the presence of I_2 in the solution after reaction over $\text{I-Pd/Al}_2\text{O}_3$ by a test with addition of starch. The solution was clear and colorless which means absence of I_2 formation (**Figure S4, SI**). Additionally, I_2 on Al_2O_3 catalyst has been prepared by impregnation of I_2 over alumina which has been used for several reactions [30-33]. However, only acetal was observed as the product of the reaction without ether formation (**Table 1, Entry 16**).

The potential application of other halogens for pretreatment of Pd has been investigated by using chlorobutane (BuCl) and bromobutane (BuBr) as additives. However, the presence of BuCl and BuBr only decreased the hydrogenation ability of $\text{Pd/Al}_2\text{O}_3$. Notably, no ether was produced over these catalysts (**Table 1, Entry 17 & 18**). CO adsorption over the catalysts after pretreatment shows similar adsorption capacity in

comparison with the parent catalyst, which indicates low adsorption of Cl and Br over Pd metal surface (Table S1, SI).

Thus, I-Pd/Al₂O₃ is an efficient and stable catalyst for reductive etherification of furfural. Moreover, we have performed the etherification reaction at even lower temperature (35 °C) for 6 h (Table 1, Entry 19) with similar activity and selectivity. Consistently, an approximate 80 % selectivity to ether product was identified by NMR analysis after the removal of non-reacted isopropanol by rotary evaporation and filtration of catalyst. ¹H and ¹³C NMR spectra of the ether are displayed in Figures S5 and S6, SI. The further purification of the product by extraction of furfural and furfuryl alcohol by water shows high purity of formed ether according to NMR analysis (Figures S7 and S8, SI) with isolated yield of 76 %. This demonstrates the practicality of this route.

Characterization of the catalyst

Deep characterization of the catalysts was performed in order to gain insights on the structure-activity relationships. HRTEM and EDS mapping analysis were carried out to identify the changes after modification of EtI and preferred location of the iodine species on the I-Pd/Al₂O₃ catalyst (Figure 3, Figure S9, SI). The particle size distribution of Pd in

I-Pd/Al₂O₃ catalyst was in the range of 3 ~ 5 nm, which is similar to the parent catalyst.

According to HRTEM images, the distance between crystallographic planes was 0.225 nm, in a good agreement with the (111) lattice spacing (0.226 nm) of the face-centered cubic (fcc) Pd, which is in consistent with parent Pd/Al₂O₃ [34]. In addition, according to [Figure 3d](#), most intense iodine EDS signals come from the same locations as Pd and only negligible iodine is detected on the Al₂O₃ support. This observation suggests that most of iodine is adsorbed on the Pd surface and not on the support. Moreover, from EDS elemental analysis ([Table 2](#)), the loading of iodine on the I-Pd/Al₂O₃ catalyst is estimated to be 0.39 wt. %, which corresponds to 0.03 mmol of iodine per 1 g of catalyst.

CO chemisorption analysis of I-Pd/Al₂O₃ catalyst also suggests interaction of I species with the Pd surface atoms ([Table 2](#)). The CO uptake decreases from 0.14 mmol/g for initial Pd/Al₂O₃ to 0.0063 mmol/g for I-Pd/Al₂O₃. The dramatic decrease in the CO uptake indicates on deactivation of several Pd atoms by adsorbed I atoms. Interestingly, for the I-Pd/Al₂O₃ (N₂) and NaI-Pd/Al₂O₃ samples, the CO-adsorption uptakes did not change a lot after treatment with the iodine compounds indicating that the iodine is not effectively bonded to the Pd surface ([Table S1, SI](#)). CO-FTIR analysis was performed to

confirm the interaction of CO and Pd. [Figure S10, SI](#) shows a set of CO absorption band on initial Pd/Al₂O₃ with linear at 2090 cm⁻¹ and bridged and multiple species at 1976 cm⁻¹ and 1913 cm⁻¹, respectively [35]. However, there are no peaks of CO over I-Pd/Al₂O₃, which indicates electron withdrawing and hindrance effect of I species over Pd surface.

The electronic state of palladium and iodine in the I-Pd/Al₂O₃ catalyst was characterized by XPS. [Figure 4](#) demonstrates Pd 3d and I 3d core level spectra of I-Pd/Al₂O₃ before and after reaction compared with spectra of Pd/Al₂O₃ and PdI₂. A Pd 3d spectrum of one chemical state has 3d_{5/2} and 3d_{3/2} components with 5.26 eV spin-orbit splitting. Pd 3d spectrum of Pd/Al₂O₃ catalyst, as shown in [Figure 4a](#), has two doublets with BE (Pd 3d_{5/2}) 335.3 eV and 336.7 eV attributed to metallic Pd⁰ and Pd²⁺ (PdO) respectively [36-37]. Both of these states coexist on the surface with domination of the metallic state. A minor shift of Pd 3d peaks to higher BE for I-Pd/Al₂O₃ catalysts (both before and after reaction) can be attributed to interaction of Pd with iodine. This interaction leads to the electron withdrawal from Pd to I. In I-Pd/Al₂O₃ catalyst, Iodine has access to electrons from Pd nanoparticles resulting in lower electron density and partial positive charge of the Pd nanoparticles [38-39]. It is interesting that Pd²⁺/Pd⁰ ratio is lower for I-

Pd/Al₂O₃ sample (before reaction) comparing to that of Pd/Al₂O₃ (16% vs. 32%, [Table 2](#)).

Additional information about Pd oxidation state has been obtained from H₂-TPR analysis ([Figure S11, SI](#)). Broad peak of hydrogen consumption over Pd/Al₂O₃ is observed at 15 °C.

For the I-Pd/Al₂O₃ catalyst, a very weak reduction peak is observed at approximately 50 °C. The consumption of H₂ for Pd/Al₂O₃ and I-Pd/Al₂O₃ is 0.41 and 0.07 mmol/g, respectively ([Table 2](#)). It also points on a lower fraction of PdO phase in I-Pd/Al₂O₃ catalyst. This might suggest that I atoms coordinate over Pd surface and protect them from oxidation, preventing formation of PdO in I-Pd/Al₂O₃ catalyst.

I 3d spectra of the considered samples are shown in [Figure 4b](#), demonstrating 3d_{5/2} and 3d_{3/2} spin-orbit doublets with 11.5 eV splitting. For I-Pd/Al₂O₃ catalyst the I 3d_{5/2} peak BE is 619.5 eV. The I 3d_{5/2} peak of PdI₂ demonstrates the same BE of 619.5 eV. The I 3d_{5/2} BE for I atomically located on metal surfaces is expected between 618.5 and 619.7 eV [40]. An observed value within this region suggests dissociation of EtI over palladium. The relative broadening of I 3d peaks of I-Pd/Al₂O₃ catalyst is probably a result of irregular localization of I on the planes, edges and corners of Pd nanoparticles. I-Pd/Al₂O₃ after reaction shows similar Pd 3d and I 3d spectra suggesting high stability of the catalyst.

Mechanism of the reaction

Acetalization of carbonyl groups is usually considered as an acid catalyzed reaction and takes place in the presence of Brönsted acid sites [19-20]. Therefore, we deduce that the generation of Brönsted acid sites in the Pd-I catalysts maybe a key step for the carbonyl group activation.

To confirm the presence of Brönsted acid sites, an in-situ pyridine-FTIR analysis was carried out on Pd/Al₂O₃ and I-Pd/Al₂O₃. As shown in [Figure 5](#), after adsorption of pyridine, both initial Pd/Al₂O₃ and the I-Pd/Al₂O₃ show a peak at 1450 cm⁻¹ assigned to the Lewis acid sites probably present on the Al₂O₃ support. No peak related to the adsorption of Py over Brönsted acid sites (1540 cm⁻¹) was detected for both catalysts [41]. Then, we added hydrogen at 60 °C to check the acidity of I-Pd/Al₂O₃ close to the reaction conditions. Surprisingly, we observed appearance of a Py-IR peak at 1540 cm⁻¹. This might indicate generation of Brönsted acidity on the catalyst under hydrogen atmosphere. Removal of hydrogen from the cell led to disappearance of this peak. However, it could be recovered by dosing again hydrogen. This result indicates that the acidity generation on the Pd-I

catalyst is reversible and depends on partial pressure of hydrogen. The same experiment over parent Pd/Al₂O₃ did not show any effect of hydrogen on the catalyst acidity ([Figure 5](#)). Thus, the remarkable catalytic behavior of the I-Pd/Al₂O₃ catalysts could be explained by considering the electronic interactions between the Pd and iodine species. After dissociation of hydrogen on the surface of Pd, a strong electron withdrawing effect of the neighboring iodine species could cause polarization of hydrogen over the Pd-I pairs. Because of the high negative charge, the adsorbed iodine atoms would favor the stabilization of H⁺ produced during hydrogen dissociation resulting in the generation of Brönsted acidity. Hydrogen spillover over the Pd catalyst has been demonstrated previously [42-45]. Highly mobile hydrogen can generate Brönsted acid sites on the reducible supports such as WO₃ and CeO₂ [45]. Iglesia [46] et al in late nineties observed generation of Brönsted acidity in the presence of H₂ on WO_x-ZrO₂ catalysts with polytungstate domains. The exposure to hydrogen results in a slight reduction of tungsten and delocalization of an electron from an H atom resulting in H^{+δ} (Brönsted acid site). The catalysts developed by Iglesia are obviously rather different from our Pd-I systems. The interest and advantage of the catalytic system presented in this work is related to the

1
2
3 generation of acidity in-situ during the reaction directly on the metal sites. This Pd-I
4
5
6
7 catalyst results in the intimacy of metal and acid functions and thus, very efficient
8
9
10 bifunctional catalysts.

11
12
13
14 In order to confirm generation of acidity over Pd in the presence of hydrogen, we
15
16
17 have performed two model reactions: hydrogenation of acetone and dehydration of tert-
18
19
20 amyl alcohol (TAA) over Pd/Al₂O₃ before and after modification by EtI. [Table 3](#) shows that
21
22
23 at 200 °C the non-promoted Pd/Al₂O₃ produces isopropanol as the main product (63 %)
24
25
26 with small amount of methyl isobutyl ketone (MIBK), which is a product of aldol
27
28
29 condensation of acetone. At the same time, I-Pd/Al₂O₃ demonstrates totally different
30
31
32 catalytic performance with high selectivity to MIBK (93 %). The aldol condensation of
33
34
35 acetone proceeds over acid or basic sites. Dehydration of the product of condensation
36
37
38 leads to mesityl oxide, which is hydrogenated to MIBK [47-48]. The presence of both
39
40
41 Brönsted acid and metal sites in bifunctional catalysts such as Pd/Amberlyst-15 or
42
43
44 Pd/zeolite is essential for this reaction. I-Pd/Al₂O₃ provides both types of sites in close
45
46
47
48
49 proximity to each other, which leads to the selective synthesis of MIBK.
50
51
52
53
54
55
56
57
58
59
60

Dehydration of tert-amyl alcohol (TAA) was tested to confirm the generation of Brönsted acidity (Table 3). Notably, I-Pd/Al₂O₃ exhibited high activity and selectivity to isoamylene (Conv. 95.3% & Sel. 96.2%), while initial Pd/Al₂O₃ has low activity with formation of isopentane as the main product. This significant difference could be ascribed to the in-situ generation of strong Brönsted acid over I-Pd active sites in the presence of hydrogen [49-50].

A feasible reaction pathway for the etherification of furfural and isopropanol on the bifunctional I-Pd/Al₂O₃ catalyst is presented in Figure 1. First, Brönsted acid sites (H⁺) are produced on the sites of adsorbed iodine atoms via hydrogen dissociation on Pd-I sites. Then, the acetal intermediates are produced via nucleophilic addition of alcohol to aldehyde catalyzed by the Brönsted acid sites. The highest selectivity to acetal is observed at the beginning of the reaction and decreases with the reaction time (Figure 6). Finally, the C-O bond dissociates with formation of water and addition of H from Pd surface to form ether. This mechanism has been confirmed by isotope tracing experiment using deuterated isopropanol-d₈ as reagent (Figure S12, SI). According to the literature, one of the possible routes for the reductive etherification could be catalyzed by acid sites

via catalytic transfer hydrogenation of furfural by the MPV (Meerwein–Ponndorf–Verley) reduction with isopropanol as hydrogen donor with subsequent etherification of formed alcohol to the ether [10]. The presence of only ^1H hydrogen atom on the carbon atom in carbonyl group in furfural confirms the hydrogenolysis of grafted C-O bond and excludes the catalytic transfer hydrogenation involving deuterated isopropanol- d^8 and etherification pathway.

Other substrates

The I-Pd/ Al_2O_3 bifunctional heterogeneous catalyst was evaluated in the reductive etherification of different substrates. First, etherification of furfural with octanol also shows high selectivity to the relevant ether. This suggests that primary alcohols might be also used for the synthesis of surfactants and fuels (Table 4). Tertiary alcohol like tert-amyl alcohol has been also tested in reductive etherification of furfural (Table 4). Although the catalytic activity is relatively low in comparison with other alcohols we could observe selective formation of tert-amyl furfuryl ether. This low activity in the reaction with tertiary alcohols might be explained by difficulties in the formation of acetal-like intermediates due to steric hindrance. HMF is another valuable biomass based product. It might be easily

1
2
3 produced by dehydration of glucose and fructose. Reaction of HMF with isopropanol
4
5
6
7 leads to the synthesis of the ethers with the selectivity close to 83 %. The reductive
8
9
10 etherification of an aromatic aldehyde might also be performed with an aromatic alcohol.
11
12
13 Thus, reaction of benzyl aldehyde with benzyl alcohol leads to 80 % selectivity to benzyl
14
15
16
17 ether. The possibility of self-etherification reaction has been verified by conducting the
18
19
20 reaction without benzyl aldehyde. However, only traces of benzyl ether have been
21
22
23 produced in this case ([Figure S13, SI](#)). Substitution of an aromatic aldehyde by aliphatic
24
25
26
27 1-octanal also results in selective synthesis of ether (92 %). Acetophenone also
28
29
30 selectively reacts with methanol ([Figure S14, SI](#)). All these results demonstrate versatility
31
32
33 of the Pd-I catalyst, which can produce corresponding ethers from a variety of aldehydes
34
35
36
37 and ketones.
38
39
40
41
42
43
44

45 Conclusion

46
47
48 To conclude, modification of Pd catalysts by treatment with organic iodine
49
50
51 compounds in hydrogen leads to surface modification of Pd. The resulting Pd-I
52
53
54
55 bifunctional heterogeneous catalyst generates Brönsted acidity in-situ in the presence of
56
57
58
59
60

hydrogen. The acid sites associated with adsorbed I species and Pd metal active sites are located in close proximity over the supported Pd nanoparticles. The newly designed bifunctional heterogeneous Pd-I catalysts showed high reductive etherification activity and selectivity even at ambient temperature. Numerous aldehydes and ketones reacted on the Pd-I bifunctional catalysts with alcohols at very mild reaction conditions yielding corresponding ethers with extremely high selectivity.

Table 1. Etherification reaction of furfural over Pd catalysts treated and non-treated by iodine compounds (T=60 °C, 20 bar H₂, 0.1 g furfural, 2 g isopropanol, 50 mg catalyst, 1h)

Entry	Catalytic system	Furfural Conv., %	Selectivity, %					
			FA	THFA	Ether	Acetal	Hemiacetal	Others ^f
1	Pd/Al ₂ O ₃	87.8	0	99.1	0	0	0	0.9
2	Pd/Al ₂ O ₃ + EtI ^a	72.1	3.9	0.2	91.8	1.3	1.7	1.1
3	I-Pd/Al ₂ O ₃	35.8	0	0	83	12	1.4	3.6
4	I-Pd/Al ₂ O ₃ (N ₂) ^b	59.7	0	92.6	0	0	0	7.3
5	NaI-Pd/Al ₂ O ₃ ^c	34.5	2	83.4	0	0	0	14.6
6	Pd/Al ₂ O ₃ + iBuI ^a	92.5	7.8	0	86.2	1.3	0	4.7
7	Pd/Al ₂ O ₃ + IBn ^a	55.4	3.4	0	84.6	1.4	2.8	7.8
8	Pd/Al ₂ O ₃ + I ₂ ^a	38.2	0	0	65.6	32.7	0.5	1.2
9	I ₂ -Pd/Al ₂ O ₃	68.7	3.8	0	90	2.1	1.7	2.3
10	Pd/C	99.9	0	43.3	0	0	0	56.7

11	Pd/C + EtI ^a	88.1	19.7	1.5	69.4	0.3	2.8	6.3
12	I-Pd/C	16.8	0	0	39.7	54.5	0	5.8
13	Pd powder	52.4	8.9	90.6	0	0	0	0.5
14	Pd powder + EtI ^a	24.3	0.3	0	33.3	64.3	0	2.1
15	PdI ₂	54.8	0	0	0	99.3	0	0.7
16	I ₂ /Al ₂ O ₃ ^d	36.6	0	0	0	99.9	0	0.1
17	Pd/Al ₂ O ₃ + BuCl ^a	53.5	0	72.3	0	0	0	27.7
18	Pd/Al ₂ O ₃ + BuBr ^a	46	0	41.1	0	0	0	58.9
19	Pd/Al ₂ O ₃ + EtI ^e	99.6	7	0	82.5	0.8	6.9	2.7

^a 15 mg of EtI, iBuI, IBn, I₂, BuCl or BuBr have been added in the reaction mixture before reaction

^b Pd/Al₂O₃ was pre-treated with EtI in isopropanol under N₂ atmosphere

^c Pd/Al₂O₃ was pre-treated with NaI in water in H₂ atmosphere

^d The I₂/Al₂O₃ was prepared by impregnation method according to ref [32]

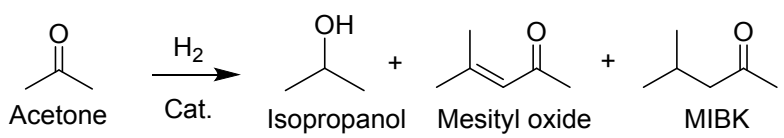
^e This experiment was performed at 35°C for 6 h

^f Others normally include tetrahydrofurfural (THFF), 2-methyltetrahydrofuran (MTHF), open rings derivatives and unknown products. Others products in some reactions (Sel. > 5%) are illustrated in Table S2, SI.

Table 2. Characterizations of Pd/Al₂O₃ and I-Pd/Al₂O₃

Catalyst	Elemental analysis, wt%		Pd ²⁺ /Pd, %	CO adsorption, mmol/g	H ₂ consumption, mmol/g	Pd _{CO} /Pd, %
	Pd	I				
Pd/Al ₂ O ₃	5	0	32	0.14	0.41	29
I-Pd/Al ₂ O ₃	5.7	0.39	16	0.0063	0.07	1.3

Table 3. Model reactions of acetone to methylbutyl ketone (2 g acetone, 50 mg catalyst, 20 bar H₂, 200 °C, 3 h) and tert-amyl alcohol dehydration (TAA) (2 g TAA, 50 mg catalyst, 10 bar H₂, 200 °C, 3 h)

				
Catalyst	Conversion of acetone (%)	Selectivity (%)		
		Isopropanol	Mesityl oxide	MIBK
Pd/Al ₂ O ₃	46.8	63.1	0	31.0
I-Pd/Al ₂ O ₃	16.1	0	2.0	93.3

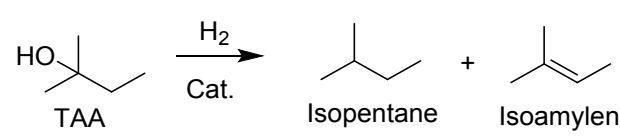
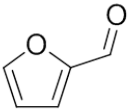
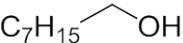
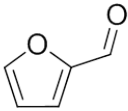
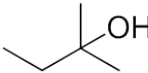
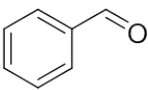
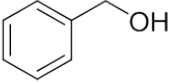
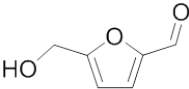
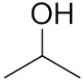
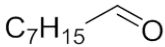
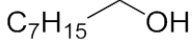
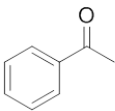

			
Catalyst	Conversion of TAA (%)	Selectivity (%)	
		Isopentane	Isoamylene
Pd/Al ₂ O ₃	7.1	99.9	0
I-Pd/Al ₂ O ₃	95.3	3.7	96.2

Table 4. Reductive etherification of various substrates (0.1 g of aldehydes or ketones, 2 g alcohols, 50 mg Pd/Al₂O₃ catalyst, 15 mg EtI were added in the reactor)

Aldehyde	Alcohol	Reaction conditions, T(°C)/t (h)/H ₂ (bar)	Conv. ^a (%)	Sel. ^b (%)
		60 / 15 / 20	95	95
		60/15/20	15	91
		60 / 15 / 20	52	80
		60 / 1 / 30	96	83 ^c
		60 / 15 / 20	96	92
		80 / 3 / 30	61	90

^a Conversion of the aldehydes or ketones

^b Selectivity to corresponding ethers

^c Summary selectivity of (5-(isopropoxymethyl)furan-2-yl)methanol and 2,5-bis(isopropoxymethyl)furan

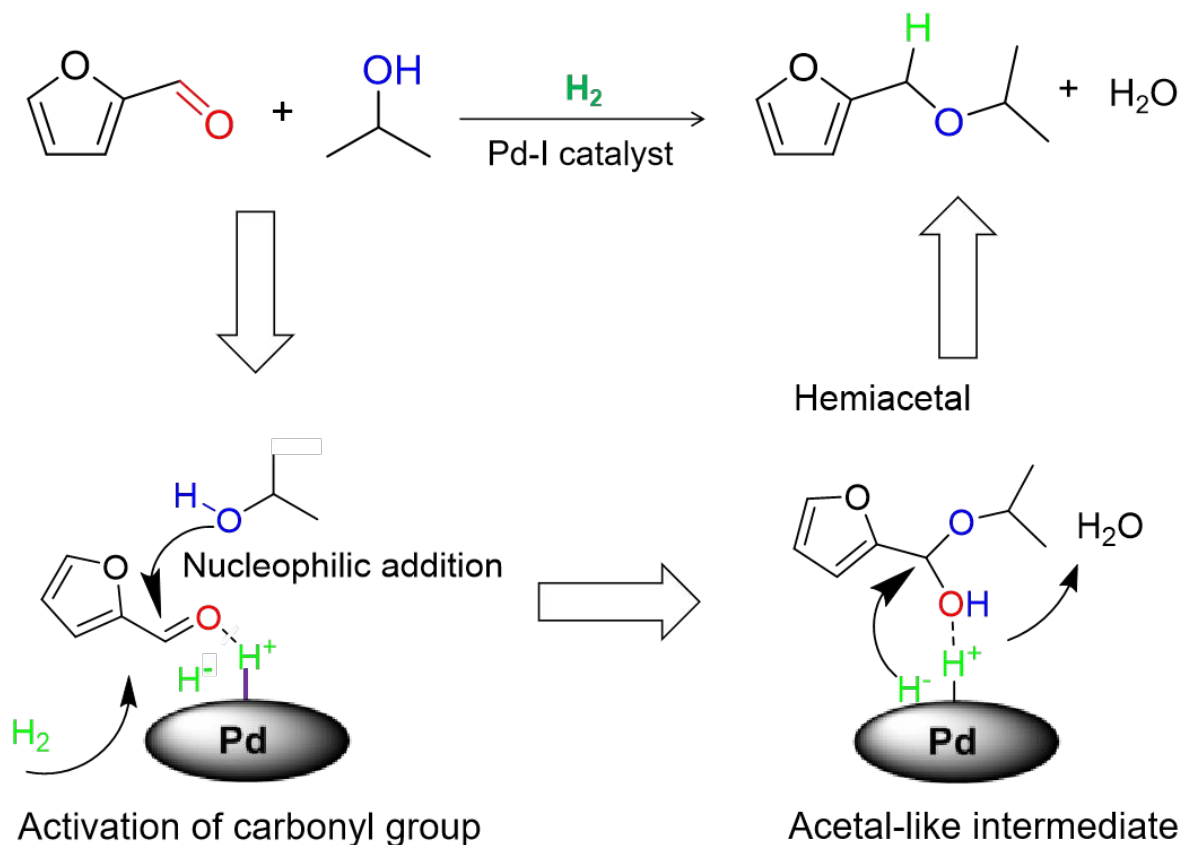


Figure 1. Scheme of the synthesis of ether from aldehyde and alcohol involving in-situ Brønsted acidity generation in the presence of hydrogen over heterogeneous Pd-I catalyst.

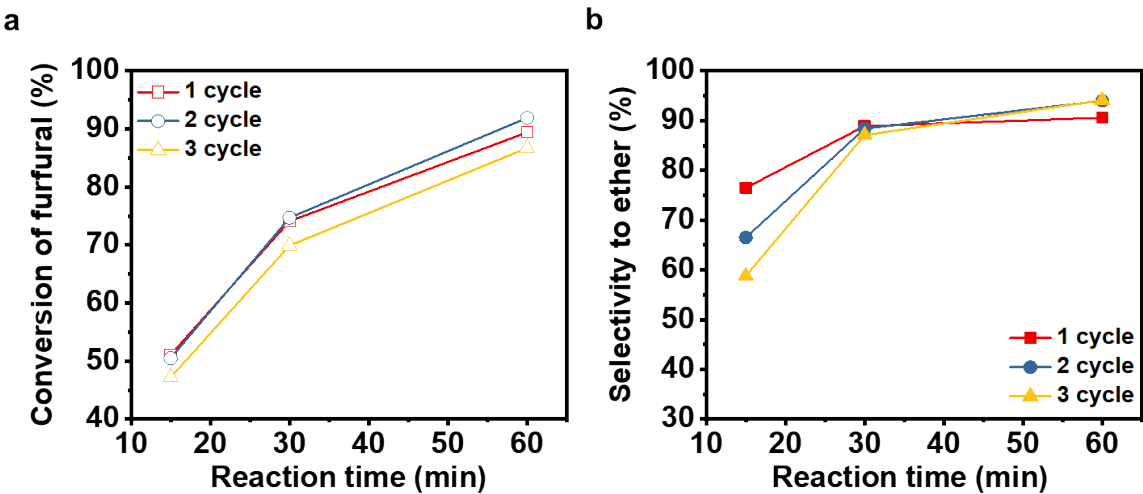


Figure 2. Evolution of conversion (a) and selectivity (b) for the first 3 cycles with reaction time. Reaction conditions: 50 mg I-Pd/Al₂O₃, 100 mg furfural, 2 g isopropanol, 60°C, 20 bar H₂.

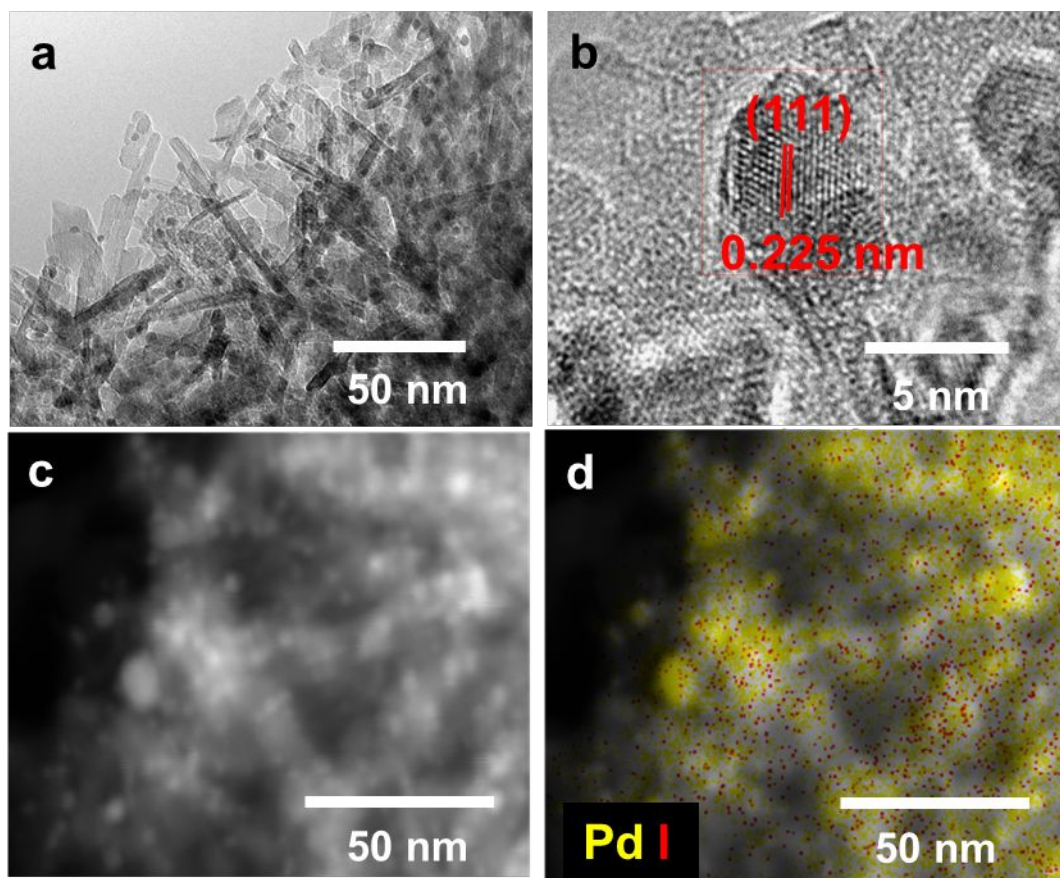


Figure 3. Characterization of I-Pd/Al₂O₃ catalyst by TEM analysis (a) TEM image; (b) HRTEM image; (c) STEM image and (d) corresponding EDS mapping image.

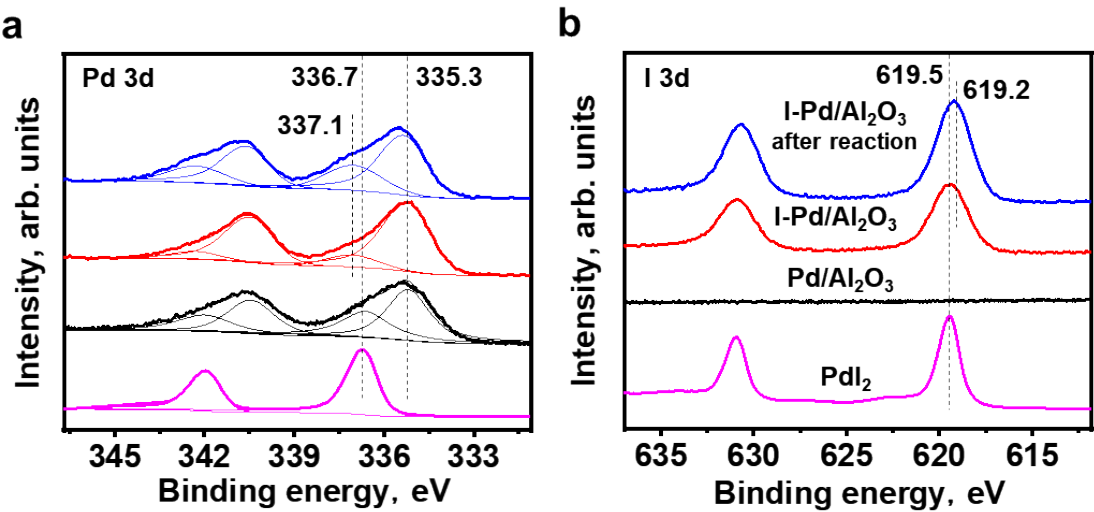


Figure 4. XPS Pd 3d (a) and I 3d (b) core level spectra of PdI₂, Pd/Al₂O₃, I-Pd/Al₂O₃, and I-Pd/Al₂O₃ after reaction.

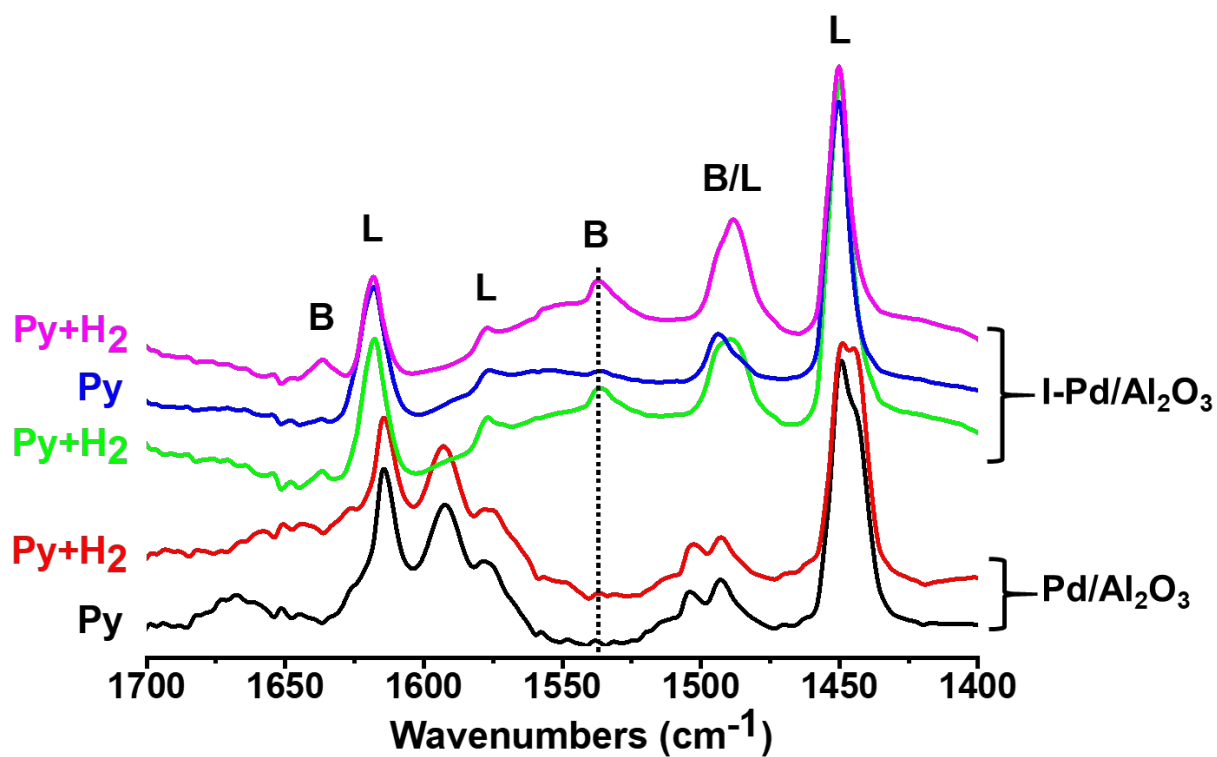


Figure 5. FTIR spectra of Py adsorption over Pd/Al₂O₃ and I-Pd/Al₂O₃ with and without hydrogen.

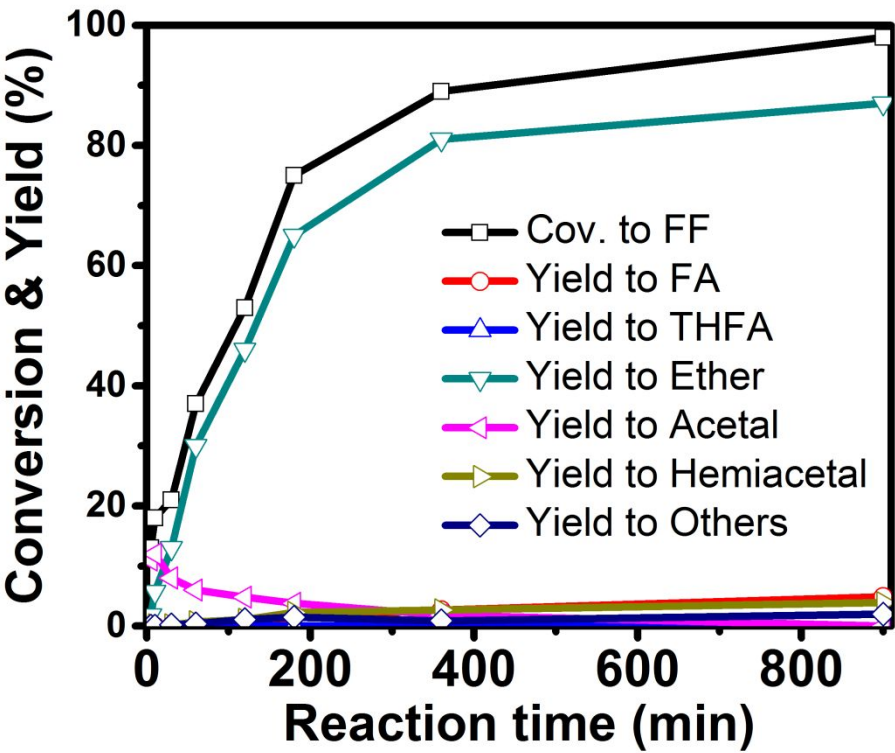


Figure 6. Evolution of conversion of furfural and yield to various products with reaction time. Reaction conditions: 25 mg of I-Pd/Al₂O₃, 200 mg of furfural, 4 g of isopropanol, 60 °C, 20 bar H₂.

ASSOCIATED CONTENT

Supporting Information. Materials; Preparation of I-Pd/Al₂O₃ (N₂), NaI-Pd/Al₂O₃, I₂-Pd/Al₂O₃ and I₂/Al₂O₃; Photos of reaction liquid during reaction process; GC and GC-MS images; Tables for CO adsorption analysis and description of side-products.

AUTHOR INFORMATION

Corresponding Author

Andrei Khodakov: E-mail:andrei.khodakov@univ-lille.fr;

Unité de Catalyse et de Chimie du Solide

UMR 8181 CNRS, Ecole Centrale de Lille, Université de Lille

Bât. C3, 59655 Villeneuve d'Ascq, France

Vitaly Ordonsky: E-mail:vitaly.ordonsky-ext@solvay.com

E2P2L, UMI 3464 CNRS-Solvay, 3966 Jin Du Rd., 201108 Shanghai, China

Author Contributions

The manuscript was written through contributions of all authors. All authors have given approval to the final version of the manuscript.

ACKNOWLEDGMENT

Dan Wu thanks Solvay and Lille University for stipend for PhD research.

REFERENCES

[1] Corma, A.; Iborra, S.; Velty, A. Chemical Routes for the Transformation of Biomass into Chemicals. *Chem. Rev.* **2007**, *107*, 2411-2502.

[2] Chheda, J. N.; Huber, G. W.; Dumesic, J. A. Liquid-Phase Catalytic Processing of Biomass-Derived Oxygenated Hydrocarbons to Fuels and Chemicals. *Angew. Chem., Int. Ed. Engl.* **2007**, *46*, 7164-7183.

[3] Chaffey, D. R.; Davies, T. E.; Taylor, S. H.; Graham, A. E. Etherification Reactions of Furfuryl Alcohol in the Presence of Orthoesters and Ketals: Application to the Synthesis of Furfuryl Ether Biofuels. *ACS Sustainable Chem. Eng.* **2018**, *6*, 4996-5002.

[4] Feuer, H.; Hooz, J. Methods of Formation of the Ether Linkage. *In The Ether Linkage (1967)*, S. Patai ed.; **2010**.

[5] Larmier, K.; Chizallet, C.; Maury, S.; Cadran, N.; Abboud, J.; Lamic-Humblot, A. F.; Marceau, E.; Lauron-Pernot, H. Isopropanol Dehydration on Amorphous Silica-

Alumina: Synergy of Brønsted and Lewis Acidities at Pseudo-Bridging Silanols. *Angew. Chem., Int. Ed. Engl.* **2017**, *56*, 230-234.

[6] Bringue, R.; Tejero, J.; Iborra, M.; Izquierdo, J.; Fite, C.; Cunill, F. Supported Nafion Catalyst for 1-Pentanol Dehydration Reaction in Liquid Phase. *Chem. Eng. J.* **2008**, *145*, 135-141.

[7] Williamson, A. W., XXII.-On etherification. *Quarterly Journal of the Chemical Society of London* **1852**, *4*, 229-239.

[8] Dermer, O. C. Metallic Salts of Alcohols and Alcohol Analogs. *Chem. Rev.* **1934**, *14*, 385-430.

[9] Balakrishnan, M.; Sacia, E. R.; Bell, A. T. Etherification and Reductive Etherification of 5-(Hydroxymethyl)furfural: 5-(Alkoxymethyl)furfurals and 2,5-Bis(alkoxymethyl)furans as Potential Bio-diesel Candidates. *Green Chem.* **2012**, *14*, 1626-1634.

[10] Shinde, S.; Rode, C. Cascade Reductive Etherification of Bioderived Aldehydes over Zr-Based Catalysts. *ChemSusChem* **2017**, *10*, 4090-4101.

[11] Jadhav, D.; Grippo, A. M.; Shylesh, S.; Gokhale, A. A.; Redshaw, J.; Bell, A. T. Production of Biomass-Based Automotive Lubricants by Reductive Etherification. *ChemSusChem* **2017**, *10*, 2527-2533.

[12] Zhao, C.; Sojda, C. A.; Myint, W.; Seidel, D. Reductive Etherification via Anion-Binding Catalysis. *J. Am. Chem. Soc.* **2017**, *139*, 10224-10227.

[13] Nguyen, H.; Xiao, N.; Daniels, S.; Marcella, N.; Timoshenko, J.; Frenkel, A.; Vlachos, D. G. Role of Lewis and Brønsted Acidity in Metal Chloride Catalysis in Organic Media: Reductive Etherification of Furanics. *ACS Catal.* **2017**, *7*, 7363-7370.

[14] Jennifer, D. L.; Stijn, V. V.; Anthony, J. C.; William, R. G.; Vladimir, K. M.; Robert, G. G.; Yuriy, R. L. A Continuous Flow Strategy for the Coupled Transfer Hydrogenation and Etherification of 5-(Hydroxymethyl)furfural using Lewis Acid Zeolites. *ChemSusChem* **2014**, *7*, 2255-2265.

[15] Jungho, J.; Eyas, M.; Raul, F. L.; Dionisios; G. V. Cascade of Liquid-Phase Catalytic Transfer Hydrogenation and Etherification of 5-Hydroxymethylfurfural to Potential Biodiesel Components over Lewis Acid Zeolites. *ChemCatChem* **2014**, *6*, 508-513.

[16] Wang, Y.; Cui, Q.; Guan, Y.; Wu, P. Facile Synthesis of Furfuryl Ethyl Ether in High Yield via the Reductive Etherification of Furfural in Ethanol over Pd/C under Mild Conditions. *Green Chem.* **2018**, *20*, 2110-2117.

[17] Basu, M. K.; Samajdar, S.; Becker, F. F.; Banik, B. K. A New Molecular Iodine-Catalyzed Acetalization of Carbonyl Compounds. *Synlett.* **2002**, 319-321.

[18] Yoshimura, A.; Zhdankin, V. V. Advances in Synthetic Applications of Hypervalent Iodine Compounds. *Chem. Rev.* **2016**, *116*, 3328-435.

[19] Breugst, M.; von der Heiden, D. Mechanisms in Iodine Catalysis. *Chemistry* **2018**, *24*, 9187-9199.

[20] von der Heiden, D.; Bozkus, S.; Klussmann, M.; Breugst, M. Reaction Mechanism of Iodine-Catalyzed Michael Additions. *J. Org. Chem.* **2017**, *82*, 4037-4043.

[21] Kahsar, K. R.; Schwartz, D. K.; Medlin, J. W. Control of Metal Catalyst Selectivity through Specific Noncovalent Molecular Interactions. *J. Am. Chem. Soc.* **2014**, *136*, 520-526.

[22] Liu, P.; Qin, R.; Fu, G.; Zheng, N. Surface Coordination Chemistry of Metal Nanomaterials. *J. Am. Chem. Soc.* **2017**, *139*, 2122-2131.

[23] Zhang, J.; Ellis, L. D.; Wang, B.; Dzara, M. J.; Sievers, C.; Pylypenko, S.; Nikolla, E.; Medlin, J. W. Control of Interfacial Acid-Metal Catalysis with Organic Monolayers. *Nat. Catal.* **2018**, *1*, 148-155.

[24] Lange, J. P. Renewable Feedstocks: The Problem of Catalyst Deactivation and its Mitigation. *Angew. Chem., Int. Ed. Engl.* **2015**, *54*, 13186-13197.

[25] Liu, Q.; Bauer, J. C.; Schaak, R. E.; Lunsford, J. H. Supported Palladium Nanoparticles: An Efficient Catalyst for the Direct Formation of H₂O₂ from H₂ and O₂. *Angew. Chem., Int. Ed. Engl.* **2008**, *47*, 6221-6224.

[26] Zaera, F. Preparation and Reactivity of Alkyl Groups Adsorbed on Metal Surfaces. *Acc. Chem. Res.* **1992**, *25*, 260-265.

[27] Beatriz, C. B.; Susan, L. M.; Manuel, P. S. Anodic Underpotential Deposition and Cathodic Stripping of Iodine at Polycrystalline and Single-crystal Gold Studies by LEED, AES, XPS, and Electrochemistry. *J. Phys. Chem.* **1991**, *95*, 5245-5249.

[28] Ayyoub, S.; Natalie, A. L.; Delphine, F.; Olivier, C.; Farid, C.; Mohamed, T. A Comparative Study of Solvent-Free and Highly Efficient Pinene Hydrogenation over Pd on Carbon, Alumina, and Silica Supports. *Org. Process Res. Dev.* **2017**, *21*, 60-64.

[29] Joyee, M.; Xiaoyuan, Z.; Thomas, R. Pd/C-Catalyzed Reactions of HMF: Decarbonylation, Hydrogenation and Hydrogenolysis. *Green Chem.* **2015**, *17*, 307-313.

[30] Richard, M. P.; George, W. K.; Richard, B.; Kevan, G.; Lyman, J. S.; Richard, C.; Christopher, D.; Donna, G.; Steven, L.; Teresa, L. Reactions of Unsaturated Compounds with Iodine and Bromine on γ Alumina. *J. Org. Chem.* **1988**, *53*, 4477-4482.

[31] Md, R. R.; Mantu, R.; Badaker, M. L.; Priti, R. S.; Bekington, M. Iodine-Alumina as an Efficient and Useful Catalyst for the Regeneration of Carbonyl Functionality from the Corresponding 1,3-Oxathiolanes and. 1,3-Dithiolanes in Aqueous System. *Tetrahedron Lett.* **2010**, *51*, 2862-2864.

[32] Nabajyoti, D.; Jadab, C. S. Highly Efficient Dithioacetalization of Carbonyl Compounds Catalyzed with Iodine Supported on Neutral Alumina. *Chem. Lett.* **2001**, *30*, 794-795.

[33] Ira, S.; Dilip, C. B.; Jadab, C. S. Three Component Condensations Catalyzed by Iodine-Alumina for the Synthesis of Substituted 3,4-Dihydropyrimidin-2(1H)-ones under Microwave Irradiation and Solvent-Free Conditions. *Tetrahedron Lett.* **2005**, *46*, 1150-1160.

[34] Xiong, Y.; Cai, H.; Wiley, B. J.; Wang, J.; Kim, M. J.; Xia, Y. Synthesis and Mechanistic Study of Palladium Nanobars and Nanorods. *J. Am. Chem. Soc.* **2007**, *129*,

3665-3675.

[35] Benkhaleda, M.; Morin, S.; Pichon, Ch.; Thomazeau, C.; Verdon, C.; Uzio, D. Synthesis of Highly Dispersed Palladium Alumina Supported Particles: Influence of the Particle Surface Density on Physico-Chemical Properties. *Appl. Catal., A*. **2006**, *312*, 1-11.

[36] Bhogeswararao, S.; Srinivas, D. Catalytic Conversion of Furfural to Industrial Chemicals over Supported Pt and Pd Catalysts. *J. Catal.* **2015**, *327*, 65-77.

[37] Yong, W.; Jia, Y.; Haoran, Li.; Dangsheng, Su.; Markus, A. Highly Selective Hydrogenation of Phenol and Derivatives over a Pd@Carbon Nitride Catalyst in Aqueous Media. *J. Am. Chem. Soc.* **2011**, *133*, 2362-2365.

[38] Komanoya, T.; Kinemura, T.; Kita, Y.; Kamata, K.; Hara, M. Electronic Effect of Ruthenium Nanoparticles on Efficient Reductive Amination of Carbonyl Compounds. *J. Am. Chem. Soc.* **2017**, *139*, 11493-11499.

[39] Nieminen, V.; Honkala, K.; Taskinen, A.; Murzin, D. Y. Intrinsic Metal Size Effect on Adsorption of Organic Molecules on Platinum. *J. Phys. Chem. C* **2008**, *112*, 6822-6831.

[40] Kovh, I.; Solymosi, F. Thermal and Photoinduced Dissociation of C₂H₅I To Yield C₂H₅ on a Pd(100) Surface. *J. Phys. Chem.* **1993**, *97*, 11056-11063.

[41] An, J.; Wang, Y.; Lu, J.; Zhang, J.; Zhang, Z.; Xu, S.; Liu, X.; Zhang, T.; Gocyla, M.; Heggen, M.; Dunin-Borkowski, R. E.; Fornasiero, P.; Wang, F. Acid-Promoter-Free

Ethylene Methoxycarbonylation over Ru-Clusters/Ceria: The Catalysis of Interfacial Lewis Acid–Base Pair. *J. Am. Chem. Soc.* **2018**, *140*, 4172-4181.

[42] Yang, R. T.; Wang, Y. Catalyzed Hydrogen Spillover for Hydrogen Storage. *J. Am. Chem. Soc.* **2009**, *131*, 4224-4226.

[43] Du, A. J.; Smith, S. C.; Yao, X. D.; Lu, G. Q. Hydrogen Spillover Mechanism on a Pd-Doped Mg Surface as Revealed by ab initio Density Functional Calculation. *J. Am. Chem. Soc.* **2007**, *129*, 10201-10204.

[44] Conner, W. C.; Falconer, J. L. Spillover in Heterogeneous Catalysis. *Chem. Rev.* **1995**, *95*, 759-788.

[45] Prins, R. Hydrogen Spillover. Facts and Fiction. *Chem. Rev.* **2012**, *112*, 2714-2738.

[46] David, G. B.; Max, S.; Ryan, D. W.; Stuart, L. S.; Enrique, I. Structure and Electronic Properties of Solid Acids Based on Tungsten Oxide Nanostructures. *J. Phys. Chem. B* **1999**, *103*, 630-640.

[47] Gamman, J. J.; Jackson, S. D.; Wigzell, F. A. Synthesis of Methyl Isobutyl Ketone over Pd/MgO/SiO₂. *Ind. Eng. Chem. Res.* **2010**, *49*, 8439-8443.

[48] Wang, P.; Bai, S.; Zhao, J.; Su, P.; Yang, Q.; Li, C. Bifunctionalized Hollow Nanospheres for the One-Pot Synthesis of Methyl Isobutyl Ketone from Acetone. *ChemSusChem* **2012**, *5*, 2390-2396.

[49] Gates, B. C.; Wisnouskas J. S.; Heath, H. W. The Dehydration of t-Butyl Alcohol Catalyzed by Sulfonic Acid Resin. *J. Catal.* **1972**, *24*, 320-327.

[50] Josef, M.; Chelsey, D. B.; Marcos, M. L.; Stuart, L. S.; Yong, W.; Enrique, I. Support

Effects on Brønsted Acid Site Densities and Alcohol Dehydration Turnover Rates on Tungsten Oxide Domains. *J. Catal.* **2004**, 227, 479-491.

